NANO LETTERS

2009
Vol. 9, No. 11
3689-3693

Junctions in Axial III−V Heterostructure Nanowires Obtained via an Interchange of Group III Elements

Peter Krogstrup,*,† Jun Yamasaki,‡ Claus B. Sørensen,† Erik Johnson,†,§ Jakob B. Wagner,|| Robert Pennington,|| Martin Aagesen,† Nobuo Tanaka,‡ and Jesper Nygård*,†

Nano-Science Center, Niels Bohr Institute, University of Copenhagen, Denmark, EcoTopia Science Institute, Department of Quantum Engineering, Nagoya University, 464-8603, Japan, and Center for Electron Nanoscopy, Technical University of Denmark, Denmark

Received April 28, 2009; Revised Manuscript Received September 3, 2009

ABSTRACT

We present an investigation of the morphology and composition of novel types of axial nanowire heterostructures where $Ga_xIn_{1-x}As$ is used as barrier material in InAs nanowires. Using aberration-corrected scanning transmission electron microscopy and energy dispersive X-ray analysis we demonstrate that it is possible to grow junctions by changing the group III elements, and we find that a substantial fraction of Ga can be incorporated in axial InAs/$Ga_xIn_{1-x}As$/InAs, retaining straight nanowire configurations. We explain how the adatoms are transferred to the incorporation site at the growth interface via two different routes, (1) interface diffusion and (2) volume diffusion through the catalyst particle.

Epitaxial growth of heterostructure nanowires has received increasing attention in recent years,[1−8] due to a wide range of successful applications in nanoscale electronic and optoelectronic devices.[9−12] Realization of intrawire barriers in axial III−V heterostructures is likely to play an essential part in future device applications, but so far fabrication of such barriers using binary materials has been limited to an interchange of the group V elements arsenic and phosphorus. The primary reason for this limitation is that for most materials, axial growth of heterostructures consisting of two material combinations A and B, is only possible with axial growth of either A on B or B on A, but not both.

The failure of axial growth of InAs/GaAs/InAs wires has been reported and studied intensively,[3−5] and the conclusions are that the interfacial energy between the Au-catalyst and InAs is higher than the interfacial energy between the Au-catalyst and GaAs. This prevents axial growth of InAs on GaAs as the system minimizes its free energy. This issue concerns other material combinations used for NW growth as well, and it is generally recognized that this is due to the difference in interfacial energies $\Delta\sigma = \sigma_{AC} - \sigma_{BC}$ between the catalyst particle C and the two wire materials A and B. Generally speaking, if σ_{AC} is higher than σ_{BC} axial growth of A on B fails, whereas axial growth of B on A is possible. In this argumentation the interfacial energies between the two materials A and B and between the materials and the vapor phase have been neglected, since they only play a negligible role.

If σ_{AC} and σ_{BC} are almost equal, axial growth in both directions may become possible as in the case of InP/InAs nanowires.[1] Formation of barriers in other axial heterostructures might be accessible by tuning the σ values during growth of wires with ternary compositions. To achieve effective quantum barriers, the junctions have to be well-defined in the sense that the potential landscape changes significantly over a few atomic layers. This has so far only been realized with an interchange of the group V elements. However, in this paper we have achieved well-defined junctions in nanowires by changing the group III composition along the length.

We present growth by molecular beam epitaxy (MBE) of straight nanowire heterostructures with diameters of ∼80 nm consisting of A, InAs, and B, $Ga_xIn_{1-x}As$, where x is in the range from 0 to ≈0.4. The bandgap energy as function of the GaAs mole fraction x in $Ga_xIn_{1-x}As$ is presently not known in such nanostructures, but it is reasonable to assume that it increases as function of x from the bandgap of pure InAs to the bandgap of pure GaAs like in the bulk material,[13] and we therefore use the term "barrier" for the segments

* To whom correspondence should be addressed. E-mail: (P.K.) krogstrup@fys.ku.dk; (J.N.) nygard@nbi.dk.
† University of Copenhagen.
‡ EcoTopia Science Institute, Nagoya University.
§ Department of Quantum Engineering, Nagoya University.
|| Technical University of Denmark.

10.1021/nl901348d CCC: $40.75
Published on Web 10/20/2009

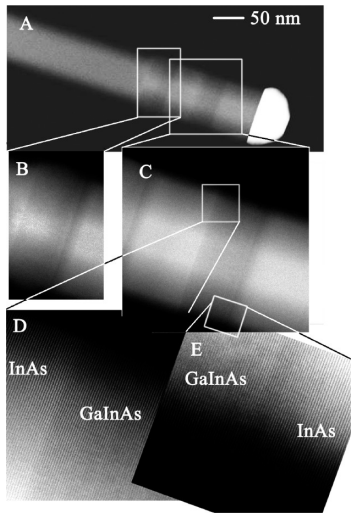

Figure 1. (A) HAADF STEM image showing a double barrier NW. The two barriers can be seen as two darker bands in the image. The blow-ups of the barriers in (B) and (C) clearly show the contrast difference between the darker $Ga_xIn_{1-x}As$ and brighter InAs regions. The sharpness of the junctions can be resolved at the atomic level in (D) for the InAs/$Ga_xIn_{1-x}As$ junction. For the $Ga_xIn_{1-x}As$/InAs junction in (E) an abrupt contrast change is followed by a more blurred transition that is typically completed within 5−10 atomic layers. These characteristics were observed on all 12 barriers characterized with HAADF STEM.

consisting of $Ga_xIn_{1-x}As$. In the present experiments, we have obtained axial growth in both directions, A−B−A with an x-value of up to ∼0.4.

The sharpness of the interfaces was determined by high resolution scanning transmission electron microscopy (HR STEM) image contrast, which is not linear although it is a monotonic function of x. For this purpose, we used an aberration-corrected high-resolution STEM (JEOL 2100F equipped with a third-order spherical aberration corrector) operated at an acceleration voltage of 200 kV. These images indicate that the $Ga_xIn_{1-x}As$/InAs junctions are abrupt, while the InAs/$Ga_xIn_{1-x}As$ junctions are somewhat broadened, see Figure 1.

However, although the atomically abrupt junction implies an instant incorporation mode of Ga at the InAs/$Ga_xIn_{1-x}As$ interface (Figure 1D), the transition from $x = 0$ to the maximum value in the barrier is from EDX data seen to be less steep at this interface than at the $Ga_xIn_{1-x}As$/InAs interface; see Figure 2. These results, which will be discussed in detail later, suggest that the incorporation of Group III materials is mediated by two distinct diffusion mechanisms, and that even though Ga only alloys weakly with the Au−In cap, a certain amount will diffuse through it during growth.

All nanowires presented here were grown by solid source molecular beam epitaxy (MBE) in a Varian GEN II MBE system. The substrates used were "epiready" InAs wafers with a (111)B As-terminated surface orientation. After thorough degassing in a separate buffer chamber, the substrates were transferred to the growth chamber and heated to 530 °C in a flux of As_2 to desorb the surface oxide. The As_2 beam equivalent pressure (BEP) used was 1.5×10^{-5} torr. After oxide removal, the substrate temperature was

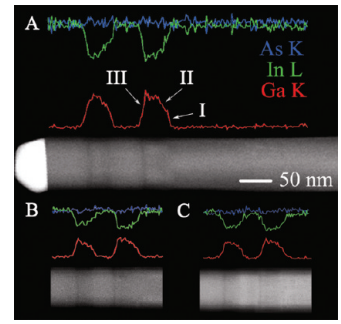

Figure 2. (A) STEM and EDX data of a double barrier nanowire with Ga mole fraction of $x \sim 0.25$. The EDX line scans show the As, In, and Ga content along the wire. The distance between the EDX steps is 1.9 nm, but we expect these data to include blurring of a few nanometers, which is due to the probe size and imperfect drift correction. At (I), a fast transition at the InAs/$Ga_xIn_{1-x}As$ junction to typically around half of the maximum value of x is observed. A slower transition to the maximum value of x appears at (II). Finally, a fast transition back to $x = 0$ is seen at the $Ga_xIn_{1-x}As$/InAs junction (III). This is the typical profile of the compositions across the junctions as seen on several single barrier wires and three different double barrier wires in (A), (B), and (C).

lowered to 490 °C and the Au was then deposited in situ directly on the oxide free surface and left to anneal in the As_2 flux for 4 min. Using the parameters above a Au deposition time of 30 s at a source temperature of 1350 °C results in wire diameters of 80 (±10) nm. Following the annealing step, the substrate temperature was lowered to the growth temperature of 423 °C.

RHEED intensity oscillation data give a measure of the bulk InAs(GaAs) growth rate as function of the temperature in the In(Ga) cell. From this we extract an expected value of the gallium mole fraction x' in the $Ga_{x'}In_{1-x'}As$ bulk material during barrier growth. The nanowires were grown using an InAs bulk growth rate of 1.5 μm/h, and for the $Ga_xIn_{1-x}As$ segments three different Ga growth rates were used, corresponding to $x' = 0.34$, 0.44, and 0.47. For all samples with only one barrier the following growth sequence was used: 20 min of InAs, 40 s of $Ga_xIn_{1-x}As$ barrier growth, 4 min of InAs, which results in nanowire lengths of around 3−4 μm. For detailed characterization of the barriers, 40 s is too much since a core−shell structure develops during $Ga_xIn_{1-x}As$ growth. All samples were cooled in an As flux after termination of the growth.

The substrate temperature of 423 °C is 31 °C below the bulk eutectic melting point temperature (BEMPT) for the Au−In alloy of 454 °C.[14] Hence, if the Au−In alloy composition is close to the eutectic point during growth we should assume a solid catalyst during growth (VSS) as described in refs 2 and 15 for InAs and GaAs nanowire growth, respectively (at the temperature used we can safely neglect phase transitions due to the Thomson-Gibbs effect[16]). In VSS growth mode the materials from the vapor phase are expected to diffuse through the solid catalyst before reaching the nucleation site at the growth interface. However, in situ TEM[17] and RHEED oscillation[18] growth studies on Au-assisted nanowire growth have shown that the state of the catalyst depends strongly on the pressure and thermal history. Liquid particles have been observed at temperatures as low as up to 70 °C below the

BEMPT for a relatively fast decrease in temperature. So the possibility of this type of sustained liquid undercooling effect should be taking into account. On the other hand, a recent study[24] suggest VLS growth at 450 °C and VSS at 420 °C for InAs/InP wires. Using the same growth conditions (same annealing and cooling step prior to growth) for InAs nanowires as the wires presented here, but varying the substrate temperature we have seen that the nanowire growth rate decreases monotonically with increasing temperature and almost stops around the BEMPT. If the In content in the Au−In alloy is not significantly higher than the eutectic point during growth, it is likely that the InAs nanowire growth will have a larger growth rate with a solid catalyst than with a liquid catalyst, in contrast to for example Ge nanowire growth studied in ref 17.

In polycrystalline materials, it is well-known that the rate of atomic diffusion along interfaces generally differs significantly from the volume diffusion rate in the adjoining crystal lattices.[19,20] On the basis of the large interface to volume ratio of the nanowire growth region and on the information obtained in this study we believe that catalytic nanowire growth is not an exception. So we will distinguish between the two diffusion mechanisms of how the materials are transferred to the nucleation site at the growth interface. (1) Interface diffusion (IFD)[20] most likely occurs at the growth interface between the Au cap and the wire. However, if the catalyst is solid (VSS) other possible fast IFD paths for the adatoms could come via grain boundaries, or possible interphase boundaries,[20] within the Au-cap. Recent X-ray analyses on the Au caps terminating GaAs wires have shown several peaks from different Au−Ga structural phases after growth.[21] The structure of the narrow interface region varies with distance from the midplane, and the diffusivity will therefore be a function of distance away from the midplane.[19] As an approximation we will assume a thin plate with an effective averaged diffusivity denoted D_{IFD}. 2. Volume diffusion (VD) is referring to the atomic diffusion induced by a concentration gradient in the catalyst with an average effective diffusivity denoted D_{VD}.

The overall effective diffusivity of the incorporation system (i.e., the catalyst and growth interface) is given by

$$D \approx \eta D_{IFD} + (1 - \eta) D_{VD}$$

where η is the fraction of the total diffusion time spent by the migrating atoms at the interface regions with diffusivity D_{IFD}. As the diffusion distance in materials can be approximated by $(D \times t)^{1/2}$ where t is the total diffusion time,[22] the value of the two terms ηD_{IFD} and $(1 - \eta) D_{VD}$ represents the relative amount of interface and volume diffusion respectively. We assume to have $\eta \ll 1$, but at the same time $D_{IFD} \gg D_{VD}$, and we can therefore not neglect any of the two terms a priori. So we will distinguish between the following three diffusion regimes:

A: $\eta D_{IFD} \gg (1 - \eta) D_{VD}$; under this condition the adatoms are transferred to the nucleation sites at the growth interface only along interfaces. Since D_{VD} is more temperature dependent than D_{IFD},[19] this regime is favored at sufficiently low temperatures, but also at higher η values and lower solubility of the diffusant in the catalyst material.

B: $\eta D_{IFD} \approx (1 - \eta) D_{VD}$, here both diffusion processes contribute to the nanowire growth.

C: $\eta D_{IFD} \ll (1 - \eta) D_{VD}$ this volume diffusion regime is favored at higher temperatures, lower η values and higher solubility of the diffusant in the catalyst material.

It is known that the solubility of As in Au is very low,[2] and therefore we assume this element to be a diffusant of regime A at low growth temperatures. This assumption is supported by studies on InAs/InP[1] and GaAs/GaP[23] nanowires, where the exchange of As and P occurs instantly at lower temperatures, giving abrupt junctions. On the other hand, recent EDX measurements on InAs/InP wires[24] indicate that there might be a considerable amount of As in the catalyst during growth at higher temperatures. The solubilities of both Ga and In in Au are known to be high although they will depend on the growth conditions, making the system more complex. However, by selecting appropriate growth parameters it may be possible to have a situation where the solubility of one of the elements in the Au particle is much higher than the other, thus providing equilibrium conditions where only one element will alloy with the Au particle. EDX measurements that have been carried out on InAs nanowires terminated by growth of ~150 nm of GaAs below the Au cap and grown under the same conditions as the barrier wires presented here have shown that the Au cap contained about 20−30% In and virtually no Ga; the results of which are confirmed by another study.[5] This is an indication of either a low solubility of Ga in Au during growth in the presence of In or that Ga may be released from the Au cap during cooling after growth.

The HAADF STEM images of the junctions (Figure 1D,E) and the typical EDX composition profiles seen in Figure 2 suggest that the Ga adatoms under these growth conditions are diffusants of type B.

In the case of solely VD growth (regime C), the InAs/$Ga_xIn_{1-x}As$ junction is expected to be blurred since Ga needs to be incorporated in the Au−In-cap before incorporation in the wire, and therefore the Ga content in the wire will increase until a steady state Au−In−Ga solution is established in the catalyst during growth. After termination of $Ga_xIn_{1-x}As$ growth, a blurred $Ga_xIn_{1-x}As$/InAs junction is also expected since Ga needs to be released from the Au cap before pure InAs growth can take place. However, studies on GaAs/InAs NW heterointerfaces[5] show that when the Au−Ga alloyed catalyst is exposed to the In flux, the catalyst quickly changes its composition by expelling Ga and absorbing In, where in the opposite case In tends to stay in the catalyst. These differences suggest that In might have more thermodynamic affinity toward Au than Ga, and tell us that the $Ga_xIn_{1-x}As$/InAs junction will be completed faster than the InAs/$Ga_xIn_{1-x}As$ junction.

In the case of solely IFD growth (regime A), Ga will be incorporated instantaneously as in the case of As and therefore both junctions are expected to be atomically abrupt.

For the wires with short barriers and no core−shell structure the EDX data show that the transition from the minimum to the maximum value of x in the barrier was slightly slower at the InAs/$Ga_xIn_{1-x}As$ interface than at the

$Ga_xIn_{1-x}As$/InAs interface. High resolution STEM images of the InAs/$Ga_xIn_{1-x}As$ interface on the other hand, show that a substantial compositional change happens at the atomic level. These informations indicate that both incorporation modes for Ga are present, and Ga therefore is a diffusant of regime B. From the EDX data, we estimate the fraction of Ga incorporated from the two mechanisms to be comparable, as the width of the transition zone from $x = 0$ to typically around half of the maximum value in the barrier is below the lateral EDX resolution. HR HAADF STEM images of the $Ga_xIn_{1-x}As$/InAs junction (see Figure 1E) also show a slightly darker band with higher concentration of Ga, followed by a slight decrease in intensity over typically the following 5−10 atomic layers. This may be an indication that a small amount of Ga is left in the catalyst after barrier growth, and that this Ga is incorporated in the wire shortly after the beginning of InAs growth. Other sources may also contribute to this profile such as surface segregation, as observed in bulk $Ga_xIn_{1-x}As$/GaAs interfaces,[25] but this contribution must be small since we would expect to see similar segregation effects at the InAs/$Ga_xIn_{1-x}As$ junction. On the basis of the NWs presented here, it is difficult to say which diffusion regime indium belongs to, but the higher thermodynamic affinity of In in Au relative to Ga, suggest that In is somewhere in between regime B and C.

The Ga mole fraction x was determined as the average x-value in the barrier region by EDX analysis (see Supporting Information on the EDX analysis).They showed in all cases a lower concentration of Ga in the barrier region than expected from the bulk growth rate calibration. The wires are distributed randomly on the substrate and the local wafer area from which a single wire collects material for its growth (with different diffusion lengths) is different for each individual wire. Therefore determining a reliable relationship between x' and x, requires more statistics. However, using scanning electron microscopy (SEM) images (see Figure 4), we can see an increasing number of kinked wires as x' is increased and thereby estimate an upper limit of the threshold value for straight barrier growth. The abundance of kinked wires has been determined by counting over a large area of each sample, and in Figure 4D the fraction of kinked wires has been plotted as function of x'. If all wires had exactly the same growth conditions within a given sample we would expect the majority of all wires to be either straight or kinked, depending on whether the x'-value is either under or over the threshold value, respectively. Because of the large difference in the surface diffusion lengths between In and Ga,[26,27] with In being the more mobile species, it is reasonable to assume that the threshold value for x' is not smaller than x. This assumption is supported by our EDX measurements on the samples with only straight wires, where all wires had x-values lower than x'. From Figure 4D the threshold value of x' appears to be around ∼0.5, and since the highest measured x-value was ∼0.4 we roughly estimate the threshold value for x in straight wires to be between ∼0.4−0.5 for these growth conditions.

The threshold value for x and therefore also the interfacial energies may depend on parameters such as temperature and pressure used during growth. Earlier studies[3,6] have shown that these parameters have an effect on the morphology, indicating that the threshold values for x might be optimized to higher values under other growth conditions. As already mentioned, all growths presented here were done with a substrate temperature of 423 °C, a temperature that was found from optimized pure InAs nanowire growth conditions. Parameter optimization for higher threshold-values for x on these types of wires still has to be addressed.

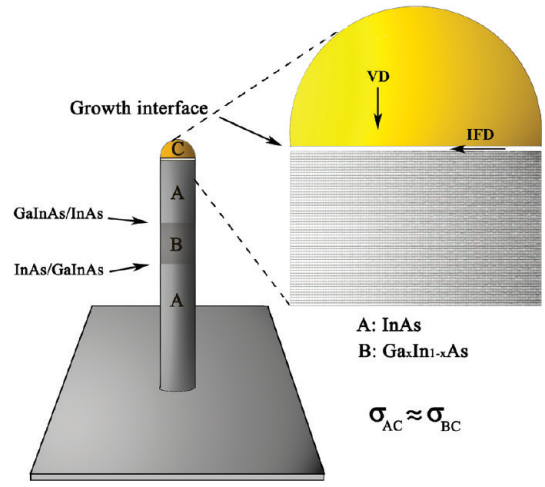

Figure 3. An illustration of an axial heterostructure nanowire. The zoom on the Au cap shows how the two types of diffusion mechanisms for the adatoms could look like at the growth region. It is likely that the IFD process occurs at the growth interface for both VLS and VSS growth modes, but also grain boundary diffusion or even phase boundary diffusion within the catalyst may play an important part if the growth mode is VSS or a combination of VLS and VSS.

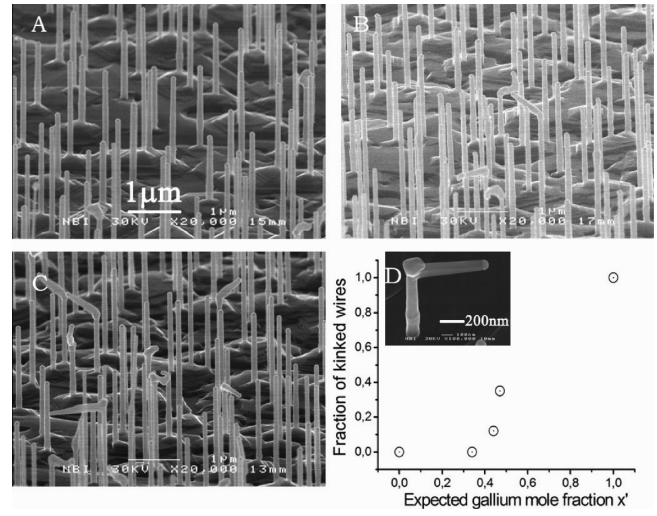

Figure 4. (A−C) SEM images of samples with $x' = 0.34$, $x' = 0.44$ and $x' = 0.47$, respectively (the scale bar in A applies also for B and C). Image A shows no kinked wires, while in image B and image C we see an increase in the fraction of kinked wires. (D) Plot of the fraction of kinked wires as a function of GaAs mole fraction x' (using the fact that all wires are straight when $x' = 0$ and all are kinked when $x' = 1$). The maximum mole fraction that can sustain axial growth is around x′≈0,5. The inset shows an image of a typical kinked wire when the amount of gallium in the barrier is too high for axial growth.

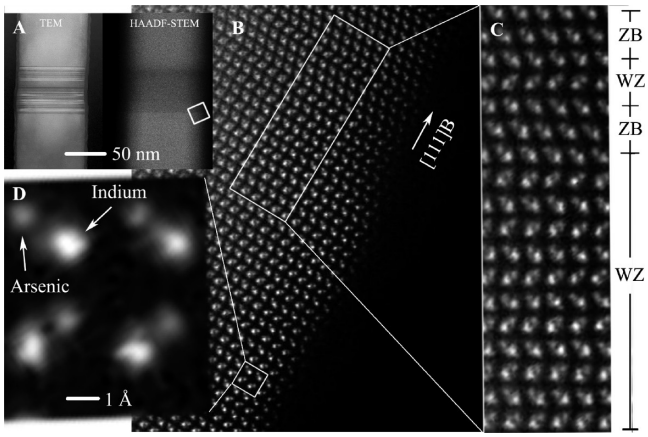

Figure 5. (A) A TEM image (left) showing structural change in the barrier region, due to a supersaturation change during growth, and a HAADF-STEM image (right) showing the compositional change in the barrier region (images from two different wires). The square in the HAADF-STEM image indicates the region corresponding to the image in (B). (B) HR-HAADF-STEM image revealing the structural composition near a barrier. (C) Close up of the structural composition cross the junction going from pure WZ in the InAs region to a interchange of WZ and ZB in the barrier. The zone axis is [01−1] (cubic). D) Zoom in (B) showing that the individual In and As columns in the InAs region with a spacing of 1.5 Å are clearly resolved by HR-HAADF-STEM. These HR images also show unambiguously that the wires grow along the [111]B direction, and that they have the same polarity as the substrate.

High supersaturation of the nanowire growth environment favors formation of the wurtzite (WZ) structure, while low supersaturation favors the zinc blende (ZB) structure.[8] The introduction of Ga gives a lower supersaturation of the environment at the growth interface, which is responsible for the high abundance of ZB segments (see Figure 5) in the barrier, in otherwise pure wurtzite (WZ) wires. Changing the growth parameters or nanowire diameters to get either pure ZB or pure WZ in the barrier is left to be done.

In conclusion, we have shown that it is possible to grow well-defined barriers in straight axial nanowires by changing the group III-components using ternary compositions. Here we have used $Ga_xIn_{1-x}As$ as the barrier material in InAs nanowires. The threshold value of the GaAs mole fraction in the barrier for successful axial barrier growth is estimated to be ~0.4−0.5 under the growth conditions presented. The width of the interfaces between $Ga_xIn_{1-x}As$ and InAs is the limiting factor for how thin barriers can be grown. We have shown that the InAs/$Ga_xIn_{1-x}As$ interface is abrupt up to a certain level of the maximum GaAs mole fraction found in the barrier. It is not possible to determine this level with high accuracy with the available characterization techniques today, but from EDX and HAADF measurements we roughly estimate it to be around half of the maximum value of x in the barrier. The $Ga_xIn_{1-x}As$/InAs junctions are estimated from HAADF images to have a width of approximately 10 atomic layers. We propose a growth model, which assumes that the route of the adatoms to the incorporation site involves two different diffusion mechanisms; an instant incorporation mode where the materials are transferred to the incorporation site via interface diffusion, and a slower incorporation mode where the group III elements diffuse through the catalyst.

Acknowledgment. The work was supported by the Danish Natural Science Research Councils. E.J. acknowledges a fellowship from The Greater Nagoya Invitation Program for International Research Scientists in Environmental Science Field operated by Chubu Science and Technology Center Foundation.

Supporting Information Available: This material is available free of charge via the Internet at http://pubs.acs.org.

References

(1) Björk, M. T.; Ohlsson, B. J.; Sass, T.; Persson, A. I.; Thelander, C.; Magnusson, M. H.; Deppert, K.; Wallenberg, L. R.; Samuelson, L. *Appl. Phys. Lett.* **2002**, *80*, 1058.
(2) Dick, K. A.; Deppert, K.; Mårtensson, T.; Mandl, B.; Samuelson, L.; Seifert, W. *Nano Lett.* **2005**, *5*, 4.
(3) Dick, K. A.; Kodambaka, S.; Reuter, M. C.; Deppert, K.; Samuelson, L.; Seifert, W.; Wallenberg, L. R.; Ross, F. M. *Nano Lett.* **2007**, *7*, 6.
(4) Paladugu, M.; Zou, J.; Guo, Y. N.; Auchterlonie, G. J.; Joyce, H. J.; Gao, Q.; Tan, H. H.; Jagadish, C.; Kim, Y. *Small* **2007**, *3*, 7.
(5) Paladugu, M.; Zou, J.; Guo, Y.; Zhang, X.; Kim, Y.; Joyce, H. J.; Gao, Q.; Tan, H. H.; Jagadish, C. *Appl. Phys. Lett.* **2008**, *93*, 101911–1.
(6) Ohlsson, B. J.; Björk, M. T.; Persson, A. I.; Thelander, C.; Wallenberg, L. R.; Magnusson, M. H.; Deppert, K.; Samuelson, L. *Physica E* **2002**, *13*, 2–4.
(7) Regolin, I.; Sudfeld, D.; Lüttjohann, S.; Khorenko, V.; Prost, W.; Kästner, J.; Dumpich, G.; Meier, C.; Lorke, A.; Tegude, F.-J. *J. Cryst. Growth* **2007**, *298*, 607.
(8) Dheeraj, D. L.; Patriarche, G.; Zhou, H.; Hoang, T, B.; Moses, A. F.; Grønsberg, S.; van Helvoort, A. T. J.; Fimland, B. O.; Weman, H. *Nano Lett.* **2008**, *8*, 12.
(9) Björk, M. T.; Ohlsson, B. J.; Thelander, C; Persson, A. I.; Deppert, K.; Wallenberg, L. R.; Samuelson, L. *App. Phys. Lett.* **2002**, *81*, 23.
(10) Qian, F.; Gradecak, S.; Li, Y.; Wen, C.; Lieber, C. M. *Nano Lett.* **2005**, *5*, 11.
(11) Duan, X.; Huang, Y.; Agarwal, R.; Lieber, C. M. *Nature* **2003**, *421*, 241.
(12) Gudriksen, M. S.; Lauhon, L. J.; Wang, J.; Smith, D. C.; Lieber, C. M. *Nature* **2002**, *415*, 617.
(13) Singh, J. Properties of lattice-matched and strained InGaAs. *Inspec*; Bhattacharya, P, Ed.; Inspec: London, 1993; Emis Datareviews series No.8, Chapter 3.
(14) Massalski, T. B.; Murray, J. L.; Bennett, L. H.; Baker, H. *Binary Alloy Phase Diagrams*; American Society for Metals: Metals Park, OH, 1986, Vol. 1.
(15) Persson, A.; Larsson, M. W.; Stenström, S.; Ohlsson, B. J.; Samuelson, L.; Wallenberg, L. R. *Nat. Mater.* **2004**, *3*, 677–681.
(16) Porter, D. A.; Easterling, K. E. *Phase Transformations in Metals and Alloys*; Chapman & Hall: New York, 1991.
(17) Kodambaka, S.; Tersoff, J.; Reuter, M. C.; Ross, F. M. *Science* **2007**, *316*, 729.
(18) Tchemycheva, M.; Travers, L.; Patriarche, Glas, F.; Harmand, J.; Cirlin, G. E.; Dubrovskii, V. G. *J. Appl. Phys.* **2007**, *102*, 094313.
(19) Sutton, A. P.; Balluffi, R. W. *Interfaces in Crystalline Materials*; Oxford University Press: New York, 1995; Chapter 8.
(20) Kaur, I.; Mishin, Y.; Gust, W. *Fundamentals of Grain and Interphase Boundary Diffusion*, 3rd ed.; Wiley: New York, 1995; Introduction.
(21) Mariager, S. O.; Lauridsen, S. L.; Dohn, A.; Bovet, N.; Sørensen, C. B.; Schlepütz, C. M.; Willmott, P. R.; Feidenhans'l, R. *Phys. Status Solidi A* **2009**, *206, 8*, 1771–1774.
(22) Shewmon, P. *Diffusion in Solids*, 2nd ed.; TMS publications: Warrendale, PA, 1989.
(23) Borgström, M. T.; Verheijen, M. A.; Immink, G.; de Smet, T.; Bakkers, E. P. A. M. *Nanotechnology* **2006**, *17*, 4010–4013.
(24) Tizei, L. H. G.; Chiaramonte, T.; Ugarte, D.; Cotta, M. A. *Nanotechnology* **2009**, *20*, 275604.
(25) Jensen, J. R.; Hvam, J. M.; Langbein, W. *J. Appl. Phys.* **1999**, *86*, 5.
(26) Kitada, T.; Wakejima, A.; Tomita, N.; Shimomura, S.; Adachi, A.; Sano, N.; Hiyamizu, S. *J. Cryst. Growth* **1995**, *150*, 1.
(27) Sugaya, T.; Nakagawa, T.; Sugiyama, Y.; Tanuma, Y.; Yonei, K. *Jpn. J. Appl. Phys.* **1997**, *36*, 9A.

NL901348D